

Imaging Molecular Reaction and Diffusion in Organic Aerosol Particles

Peter A. Alpert^{1,*}, Pablo Corral Arroyo¹, Jing Dou², Ulrich K. Krieger², Sarah S. Steimer³, Jan-David Förster⁴, Florian Ditas⁴, Christopher Pöhlker⁴, Stéphanie Rossignol⁵, Monica Passananti⁶, Sebastian Perrier⁷, Christian George⁷, Thomas Berkemeier⁸, Manabu Shiraiwa⁹ and Markus Ammann¹.

- ¹. Laboratory of Environmental Chemistry, Paul Scherrer Institute, 5232 Villigen, Switzerland.
- ². Institute for Atmospheric and Climate Science, ETH Zürich, 8092 Zürich, Switzerland
- ³. Department of Chemistry, University of Cambridge, Cambridge, CB2 1EW, United Kingdom
- ⁴. Multiphase Chemistry Department, Max Planck Institute for Chemistry, 55128 Mainz, Germany
- ⁵. Aix Marseille Université, CNRS, LCE UMR 7376, 13331 Marseille, France
- ⁶. Department of Physics, University of Helsinki, 00014 Helsinki, Finland
- ⁷. Université Lyon 1, CNRS, UMR 5256, IRCELYON, 69626 Villeurbanne, France
- ⁸. School of Chemical & Biomolecular Engineering, Georgia Institute of Technology, Atlanta, GA 30332, United States
- ⁹. Department of Chemistry, University of California, Irvine, CA 92617, United States

* Corresponding author, peter.alpert@psi.ch.

Atmospheric aerosol particles are composed of water and a variety of inorganic and organic components stemming from natural and anthropogenic sources [1]. Airborne organic matter, in particular, can be in a highly viscous or glassy phase with properties comparable to that of a solid. It was found that water, the atmospheric solvent, diffuses through a glassy organic particle quite slowly and establishes equilibrium with relative humidity only after timescales on the order of days [2]. In addition to water, diffusion of oxidizing trace gas molecules such as O₃ through highly viscous organic aerosol can be limited and may lead to an inhomogeneous O₃ concentration and reduced chemical reaction rates compared to what is expected when assuming a homogeneous mixture [3, 4]. Reaction and diffusion kinetics of O₃ with organic shikimic acid particles was quantified in viscous organic matter using X-ray microspectroscopy however, any concentration gradients could not be visualized on spatial scale of tens of nanometers [3]. Visualizing chemical gradients due to gas-to-particle reaction would allow direct evidence of coupled molecular diffusion and reaction in aerosol particles for the first time, which we find necessary for accurate predictions of atmospheric aerosol chemical aging.

We present a study using scanning transmission X-ray microscopy coupled to near edge X-ray absorption fine structure spectroscopy (STXM/NEXAFS) to visualize the reaction of O₃ with iron to change its oxidation state in a non-reactive organic matrix, Xanthan gum, a model material for organic/biogenic marine derived particles aerosolized from the ocean surface [5]. Aerosol particles with equal mass ratio of Xanthan gum and FeCl₂ were situated in a custom environmental cell having diameters, d_p , between 0.2-2 μm . We exposed particles to O₃ at 150 ppb, relative humidity (RH) at 40%, O₂ at 40 mbar and He at 110 mbar while observing X-ray absorption at the Fe L-edge in situ. Two absorption peaks at energies corresponding to Fe^{II} and Fe^{III} were mapped with 35x35 nm spatial resolution and used to derive the fraction of Fe^{II}, α , [6] a tracer for O₃ reaction and diffusion. A kinetic multi-layer model, KM-SUB [4], was used to simulate our experiment and reproduce internal profiles of α using fit parameters which were Henry's law coefficient, H , and O₃ and Fe diffusion coefficients, D_{O_3} and D_{Fe} , respectively, in the Xanthan gum matrix. The reaction rate coefficient of O₃ with Fe^{II} in aqueous solution was $k = 8 \cdot 10^{-16} \text{ cm}^3 \text{ s}^{-1}$ from NIST Chemical Kinetics Database found at

<http://kinetics.nist.gov/solution>.

Figure 1a shows that α decreased from about 0.9 to 0.5 over the course of 4 hours. Values of α were also averaged at each t over concentric pixels from particle perimeters thus deriving 2-D vertically integrated profiles. Examples are shown in Fig. 1b and reveal that α is less at particle surfaces than at particle interiors. Model results from KM-SUB are shown which capture the general trend of O_3 reaction kinetics and corresponding chemical profiles, where $H = 5 \cdot 10^{-5} \text{ mol cm}^{-3} \text{ atm}^{-1}$, $D_{O_3} = 3 \cdot 10^{-6} \text{ cm}^2 \text{ s}^{-1}$ and $D_{Fe} = 3 \cdot 10^{-14} \text{ cm}^2 \text{ s}^{-1}$. The latter value is typical for a semi-solid material which is close in viscosity to putty. However, D_{O_3} is quite high and comparable to water self-diffusion. More data sets at higher and lower humidity should be included to better

constrain these fit parameters. A 3-D gradient in α evolving over time must have existed in order to explain our results, which could only have developed due to coupled reaction and diffusion of Fe and O_3 . We calculate the reacto-diffusive length, l , a length scale indicating the distance that O_3 molecules traveled until they reacted. Under our conditions, $l = \sqrt{D_{O_3}/(kC_{Fe^{II}})} = 9 \text{ nm}$, where $C_{Fe^{II}} = 5 \cdot 10^{21} \text{ cm}^{-3} \text{ s}^{-1}$ was the concentration of Fe^{II} . In other words, O_3 must have only penetrated tens of nanometers into the particle surface, but was completely absent in the core. If so, the observed chemical gradients must have been largely due to Fe^{II} and Fe^{III} diffusing throughout the particle. We emphasize that the e-folding time for O_3 to saturate a particle with $d_p = 1 \text{ }\mu\text{m}$ is $\tau = d_p/(4\pi D_{O_3})$ or about 3 seconds when neglecting reaction. Therefore, we strongly suggest that prediction of aerosol chemistry must consider a coupled reacto-diffusive process, which we have observed can result in an inhomogeneous internal concentration gradient over timescales of hours. However, this is highly dependent on the balance between diffusion, reaction rate and concentration of reactants in the condensed phase [7].

References:

- [1] A. Laskin *et al*, *Annu. Rev. Anal. Chem.* **9** (2016), p. 117-143.
- [2] M. Shiraiwa *et al*, *Nat. Comm.* **8** (2017), 15002.
- [3] S. S. Steimer *et al*, *Atmos. Chem. Phys.* **14** (2014), 10761-10772.
- [4] T. Berkemeier *et al*, *Phys. Chem. Chem. Phys.* **18** (2016), 12662-12674.
- [5] P. A. Alpert *et al*, *J. Geophys. Res. Atmos.* **14** (2015), 8841-8860.
- [6] R. C. Moffet *et al*, *J. Geophys. Res.* **14** (2012), D07204.
- [7] The authors acknowledge the Swiss National Science Foundation grant no. 163074, the European Union's Horizon 2020/Marie Skłodowska-Curie grant agreement no. 701647 and B. Watts, who was crucial in supporting the operation of our experimental infrastructure at the PolLux beamline.

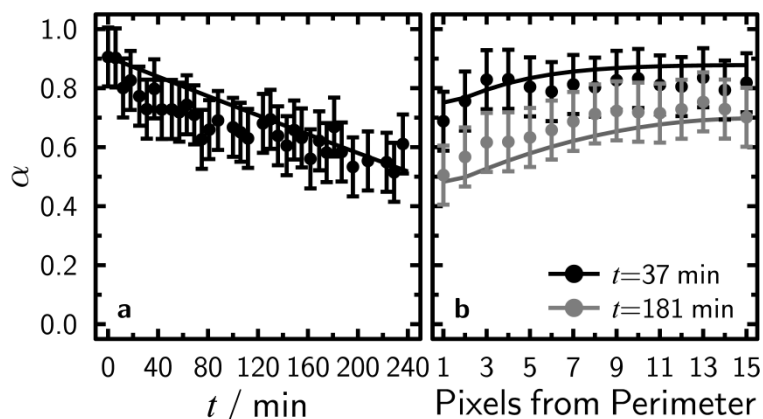


Figure 1. (a) Average Fe^{II} fraction, α , as a function of time, t . Error bars in α are ± 0.1 and calculated from the particle to particle standard deviation from the respective mean. Each data point represents the average of ~ 10 particles. (b) The 2-D projected profile of α as a function of the pixels from particle perimeters. A single profile corresponds to a single data point in t (indicated in the legend) included in panel (b). Error bars are taken from panel (a). Model results are shown as solid lines.